# Analytic Differential Admittance Operator for Tangential Dipole Illumination of a Dielectric Sphere

Martijn Huynen, Dries Vande Ginste, Daniël De Zutter and Vladimir Okhmatovski

Quantum Mechanical & Electromagnetic Systems Modelling Lab

quest.

GHENT UNIVERSITY

imec

University of Manitoba

# Boundary integral equations

## Upsides and downsides

**Boundary integral equations** (BIEs) are characterized by their use of the Green’s function and restriction of the unknowns to the boundary

This results in a smaller system matrix and automatic inclusion of the radiation condition

but in a dense matrix with more difficult numerical calculation, especially for **good** conductors

Moreover, BIEs are known to suffer from low-frequency **breakdown**, dense-mesh breakdown, internal resonances etc.

As these properties often depend on the discretization strategy, inherent analysis of the BIE’s properties is difficult

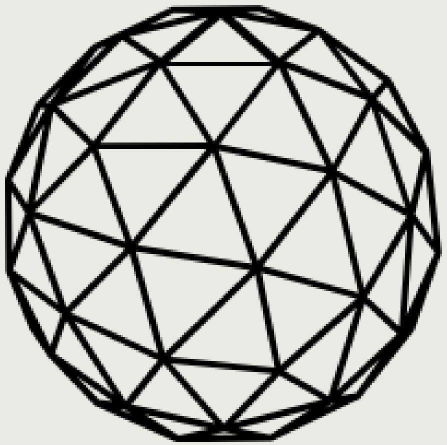

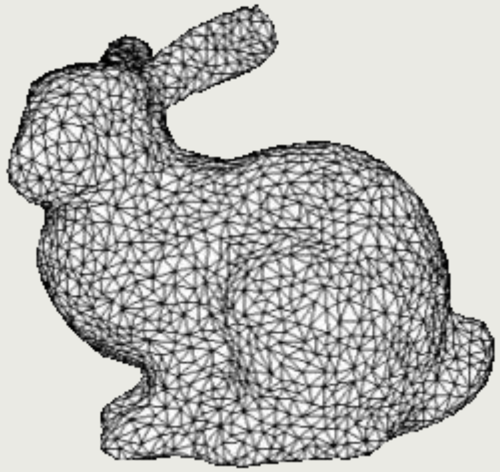

# Boundary integral equations

## Equivalence theorem

Central to all BIEs is the equivalence theorem,
which typically introduces **two** boundary sources
$\mathbf{j}_s$ and $\mathbf{m}_s$ to replace the material inside
leading to formulation such as the **PMCHWT** and **Müller BIE**

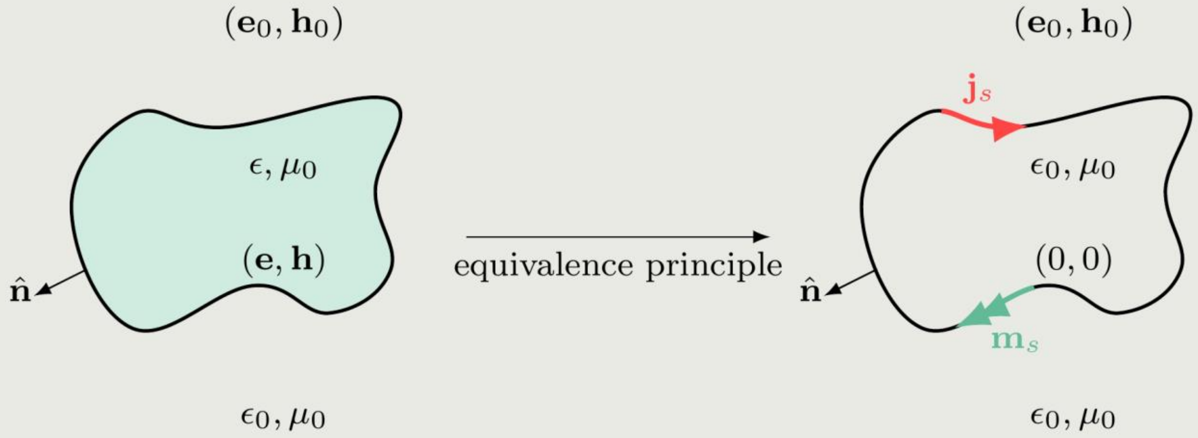


However, by giving up control over the fields inside,
a **single-source** suffices leading to formulations such as
the Surface-Volume-Surface-EFIE (**SVS-EFIE**) &
the Differential Surface Admittance-EFIE (**DSA-EFIE**)

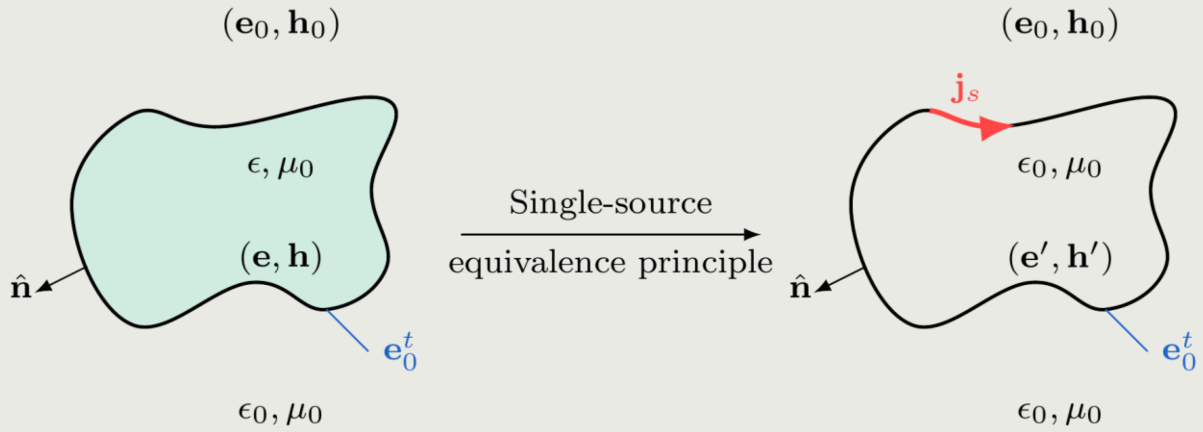


Single-source formulations typically studied less in-depth

# Boundary integral equations

## The Differential Surface Admittance operator

One way to find an expression for $\mathbf{j}_s$ , is to introduce the Poincaré-Steklov operator in both situations

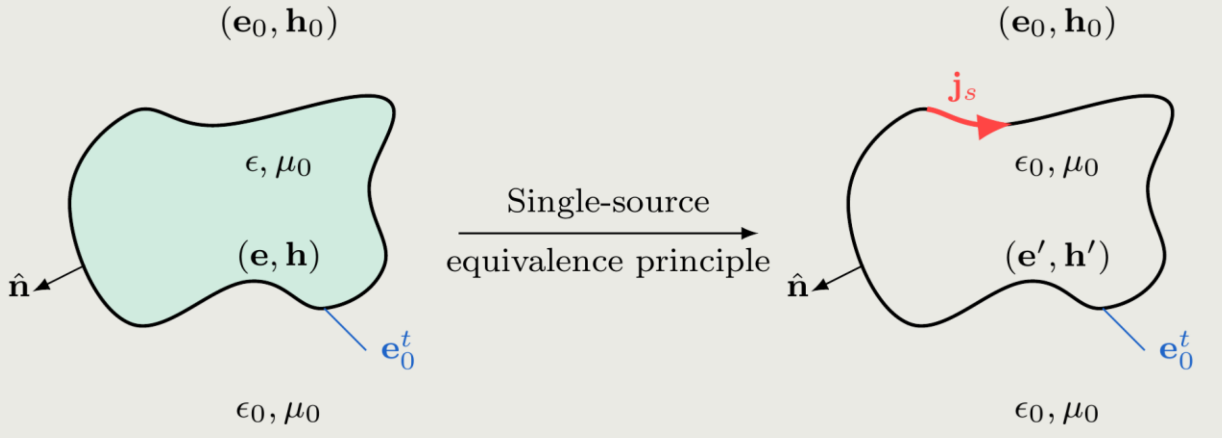


$$\hat{\mathbf{n}} \times \mathbf{h} = \mathcal{P} \circ \mathbf{e}^t \qquad \hat{\mathbf{n}} \times \mathbf{h}' = \mathcal{P}' \circ \mathbf{e}'^t$$

Imposing the boundary conditions, we then find an expression for the surface current density as

$$\mathbf{j}_s = (\mathcal{P} - \mathcal{P}') \circ \mathbf{e}_0^t = \mathcal{Y} \circ \mathbf{e}_0^t$$

# Boundary integral equations

## Applications of the DSA operator

DSA approach has been successfully applied to various problem such as

- 2-D transmission Line RLGC extraction [1]
- Arbitrary interconnect characterization [2]
- 3-D scattering & interconnects of canonical volumes [3]
- Development of magnetic interconnects [4]

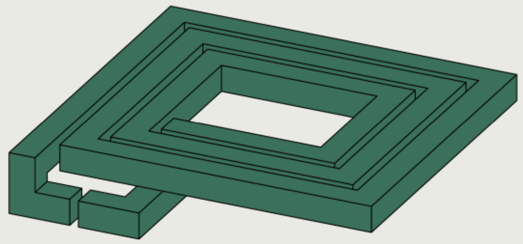

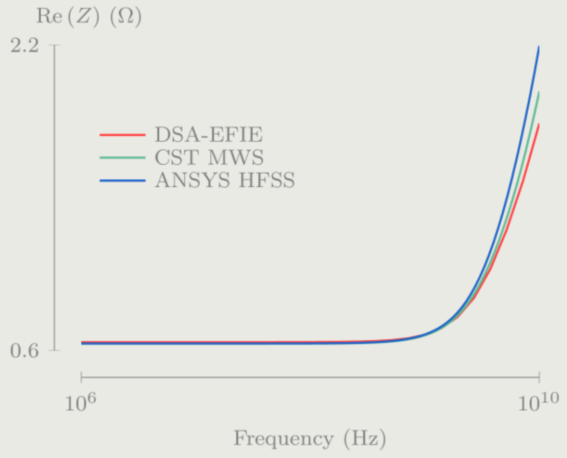


However, rigorous **proof** of the DSA's rigor, inherent properties & weaknesses, and the effects of magnetic contrast is still lacking

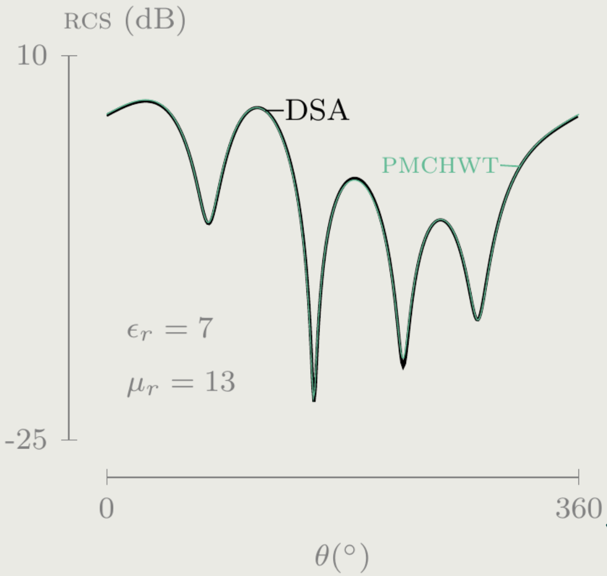


**Goal:** derive **analytical solution** for a sphere, compute **closed-form eigenvalues** and study effect **breakdown** on condition number


[1] Demeester, IEEE MTT 2008
[2] Patel, IEEE MTT 2016
[3] Huynen, IEEE MTT 2020
[4] Bosman, IEEE MTT 2023

# Spherical harmonics-based decomposition

## Boundary quantities

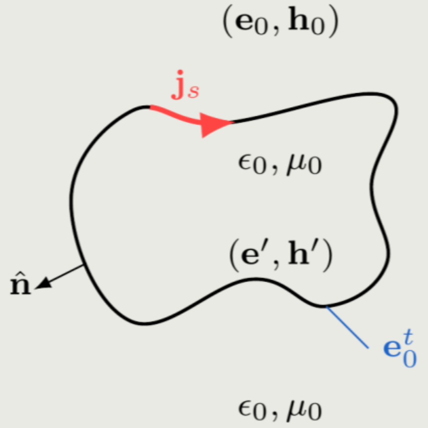


The surface current density $\mathbf{j}_s$ and tangential electric field $\mathbf{e}_0^t$ are decomposed into **two** sets of vector spherical harmonics

$\mathbf{j}_s = \alpha_{10}^{(1)}$  $+ \alpha_{20}^{(1)}$  $+ \alpha_{21}^{(1)}$ 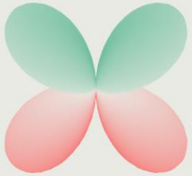 $+ \dots$

$+ \alpha_{10}^{(2)}$  $+ \alpha_{20}^{(2)}$  $+ \alpha_{21}^{(2)}$ 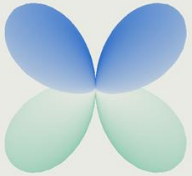 $+ \dots$

$\mathbf{e}_0^t = \beta_{10}^{(1)}$  $+ \beta_{20}^{(1)}$  $+ \beta_{21}^{(1)}$ 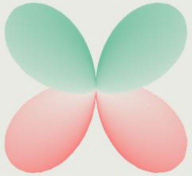 $+ \dots$

$+ \beta_{10}^{(2)}$  $+ \beta_{20}^{(2)}$  $+ \beta_{21}^{(2)}$ 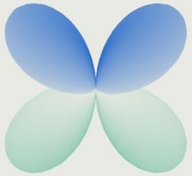 $+ \dots$

# Spherical harmonics-based decomposition

## Boundary quantities

The surface current density $\mathbf{j}_s$ and tangential electric field $\mathbf{e}_0^t$ are decomposed into **two** sets of vector spherical harmonics

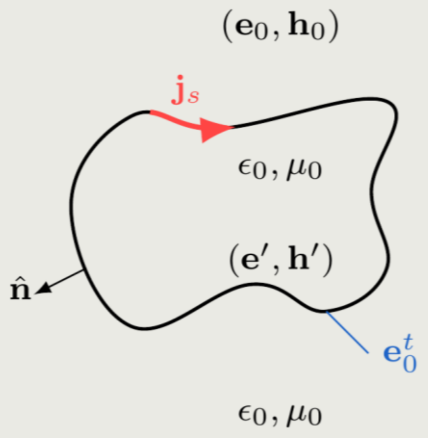


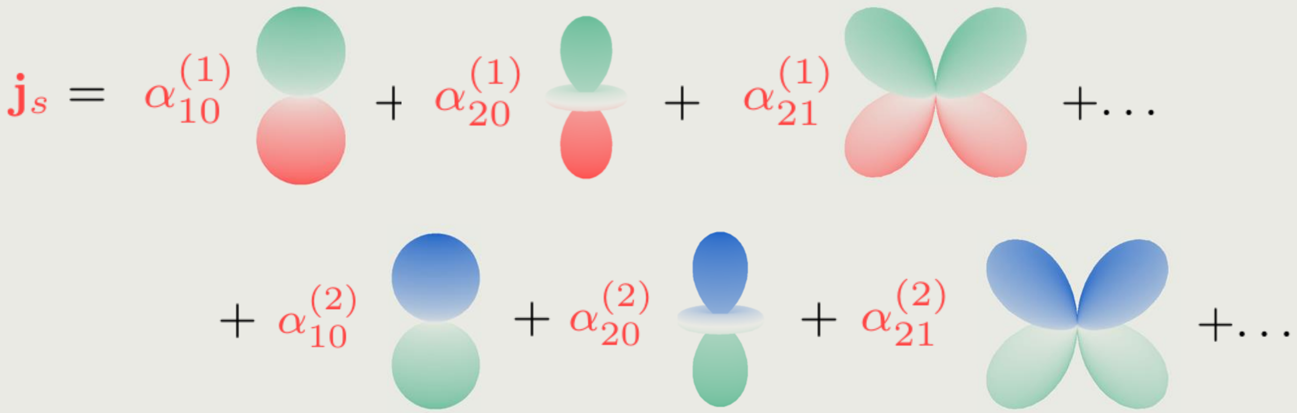


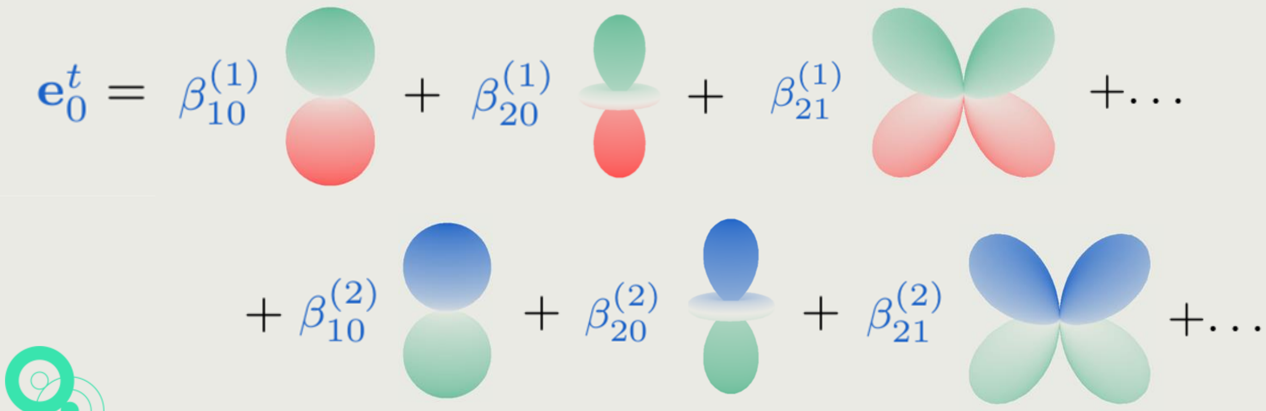


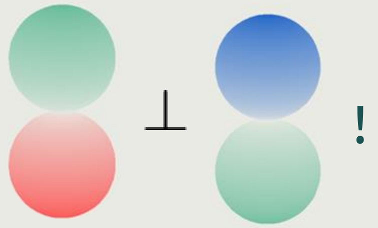

# Spherical harmonics-based decomposition

## Boundary quantities

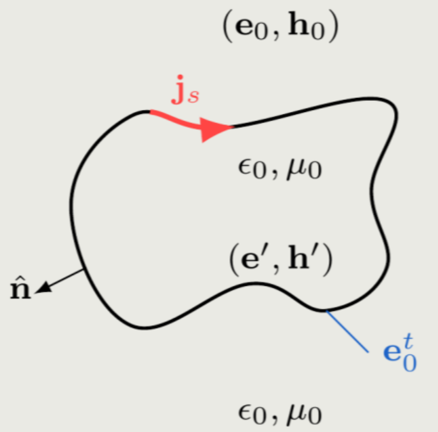


The surface current density $\mathbf{j}_s$ and tangential electric field $\mathbf{e}_0^t$ are decomposed into **two** sets of vector spherical harmonics

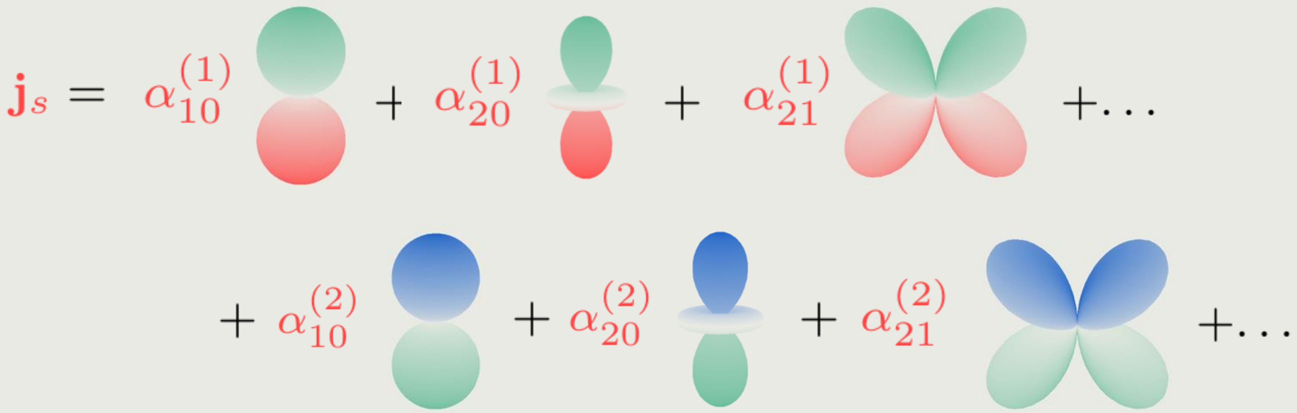


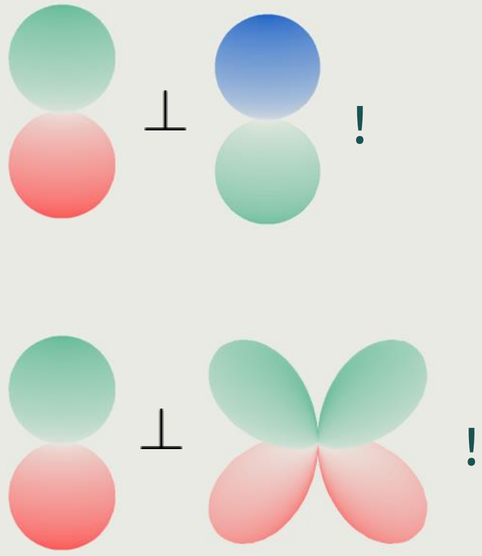


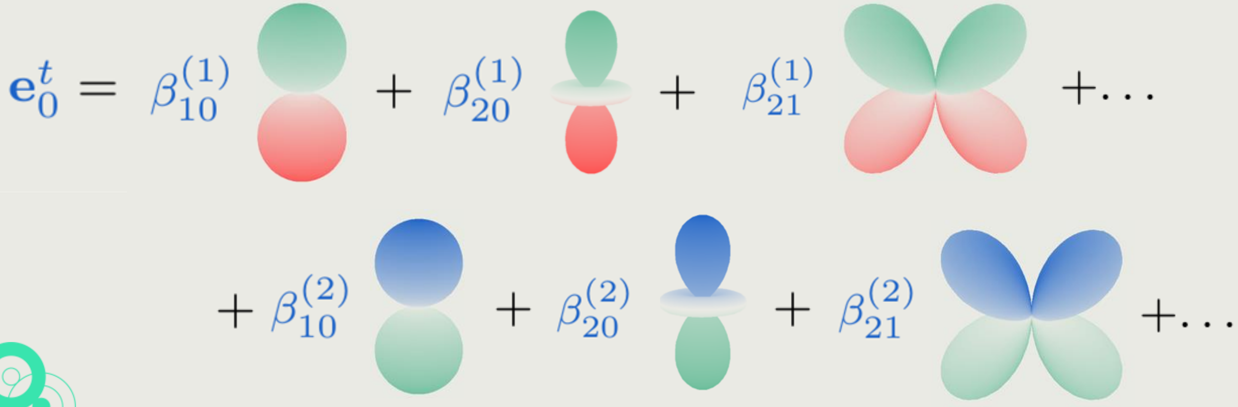

# Spherical harmonics-based decomposition

Electric Field Integral Equation (EFIE)

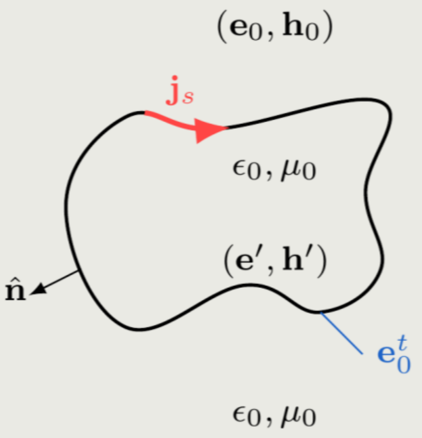


In the EFIE, the Green's kernel can be expanded into  and  well

$\beta_{10}^{(1)}$  $+\ \beta_{10}^{(2)}$  $+\dots$

$$\hat{\mathbf{n}} \times \mathbf{e}_0^t(\mathbf{r}) = \hat{\mathbf{n}} \times \mathbf{e}_{\mathrm{inc}} - j\omega\mu_0 \hat{\mathbf{n}} \times \int_{\mathcal{S}} \overline{\overline{G}}_0(|\mathbf{r} - \mathbf{r}'|)\mathbf{j}_s(\mathbf{r}')\,\mathrm{d}\mathbf{r}'$$

$\alpha_{10}^{(1)}$  $+\ \alpha_{10}^{(2)}$  $+\dots$

which, after Galerkin testing, leads to a one-to-one correspondence between every $\alpha_n^{(1)}$ and $\beta_n^{(1)}$ , and every $\alpha_n^{(2)}$and $\beta_n^{(2)}$

$$\beta_{nm}^{(1)} = \gamma_{nm} + \mathcal{Z}_n^{(1)} \alpha_{nm}^{(1)} \qquad \beta_{nm}^{(2)} = \gamma_{nm} + \mathcal{Z}_n^{(2)} \alpha_{nm}^{(2)}$$

$$\mathcal{Z}_n^{(1)} \propto [k_0 a j_n(k_0 a)]'[k_0 a h_n^{(2)}(k_0 a)]' \qquad \mathcal{Z}_n^{(2)} \propto k_0 a j_n(k_0 a)\, k_0 a h_n^{(2)}(k_0 a)$$

# Spherical harmonics-based decomposition

## Differential surface admittance operator (DSA)

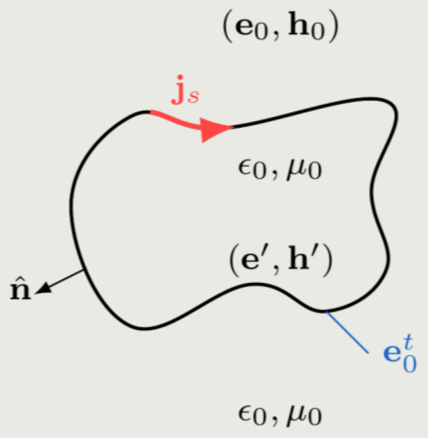


The DSA operator can be constructed in various ways to find the electric surface current density $\mathbf{j}_s$ [5], [6]

The original formulation and its 3-D extension rely on the eigenmodes of a PEC cavity and avoid the Green's function in the medium

For a sphere, the two groups of eigenmodes are of the form:

$$\mathbf{h}_{nms}^{\mathrm{TM}} \propto j_n(k_{ns} r)$$

$$\mathbf{h}_{nms}^{\mathrm{TE}} \propto j_n(k_{ns} r)$$


[5] Huynen, IEEE AWPL 2016

[6] Patel, IEEE AWPL 2017

# Spherical harmonics-based decomposition

Differential surface admittance operator (DSA)

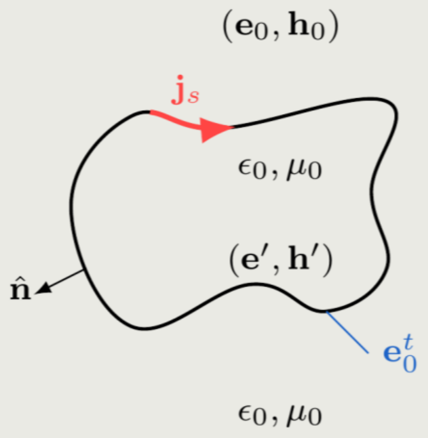


With these spherical harmonics form of the eigenmodes, we discretize

$$\mathbf{j}_s(\mathbf{r}) = -\eta \sum_{nms} \left[ \frac{\mathcal{K}_{nms}}{\mathcal{N}_{nms}^2} \int_{\mathcal{S}} (\hat{\mathbf{n}} \times \mathbf{h}_{nms}^*(\mathbf{r}')) \cdot \mathbf{e}_0^t(\mathbf{r}')\, \mathrm{d}\mathbf{r}' \right] (\hat{\mathbf{n}} \times \mathbf{h}_{nms}(\mathbf{r}))$$

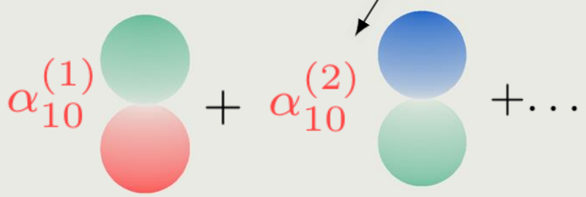


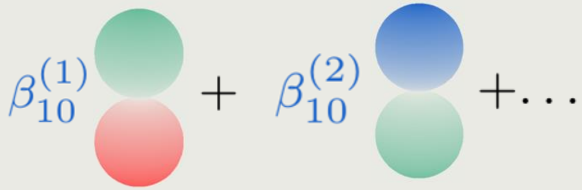


which, after Galerkin testing, leads to a one-to-one correspondence between every $\alpha_n^{(1)}$ and $\beta_n^{(1)}$, and every $\alpha_n^{(2)}$ and $\beta_n^{(2)}$

$$\alpha_n^{(1)} = \mathcal{Y}_n^{(1)} \beta_n^{(1)} \qquad \alpha_n^{(2)} = \mathcal{Y}_n^{(2)} \beta_n^{(2)}$$

$$\mathcal{Y}_n^{(1)} \propto \sum_s \frac{-2k_{ns}^2 \left(k^2 - k_0^2\right)}{\left(k_{ns}^2 - k^2\right)\left(k_{ns}^2 - k_0^2\right)\left[1 - \frac{n(n+1)}{k_{ns}^2}\right]}$$

$$\mathcal{Y}_n^{(2)} \propto \sum_s \frac{-2\kappa_{ns}^2 \left(k^2 - k_0^2\right)}{\left(\kappa_{ns}^2 - k^2\right)\left(\kappa_{ns}^2 - k_0^2\right)}$$

# Spherical harmonics-based decomposition

## Analytical solution

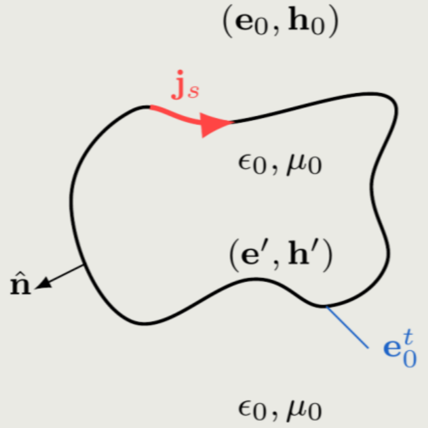


With both operators discretized and resulting in simple one-to-one relations, the system is easily solved:

$$\beta_{nm}^{(1)} = \gamma_{nm}/(1 - \mathcal{Z}_n^{(1)}\mathcal{Y}_n^{(1)}) \quad \alpha_{nm}^{(1)} = \mathcal{Y}_n^{(1)}\gamma_{nm}/(1 - \mathcal{Z}_n^{(1)}\mathcal{Y}_n^{(1)})$$

$$\beta_{nm}^{(2)} = \gamma_{nm}/(1 - \mathcal{Z}_n^{(2)}\mathcal{Y}_n^{(2)}) \quad \alpha_{nm}^{(2)} = \mathcal{Y}_n^{(2)}\gamma_{nm}/(1 - \mathcal{Z}_n^{(2)}\mathcal{Y}_n^{(2)})$$

Since the solution is fully analytical, it should be rigorous compared to the exact solution

However, the DSA elements contain an infinite sum

- Convergence rate?
- Effect different materials?
- Does it jeopardize the DSA's exactness?

# Closed-form DSA elements

## Analytical solution

The sums require the zeros of the Bessel functions, which need to be computed numerically

The sums only converge at a rate $s^{-1}$ , which is slow if machine precision is desirable

For high-contrast materials or good conductors a very slow initial convergence is observed

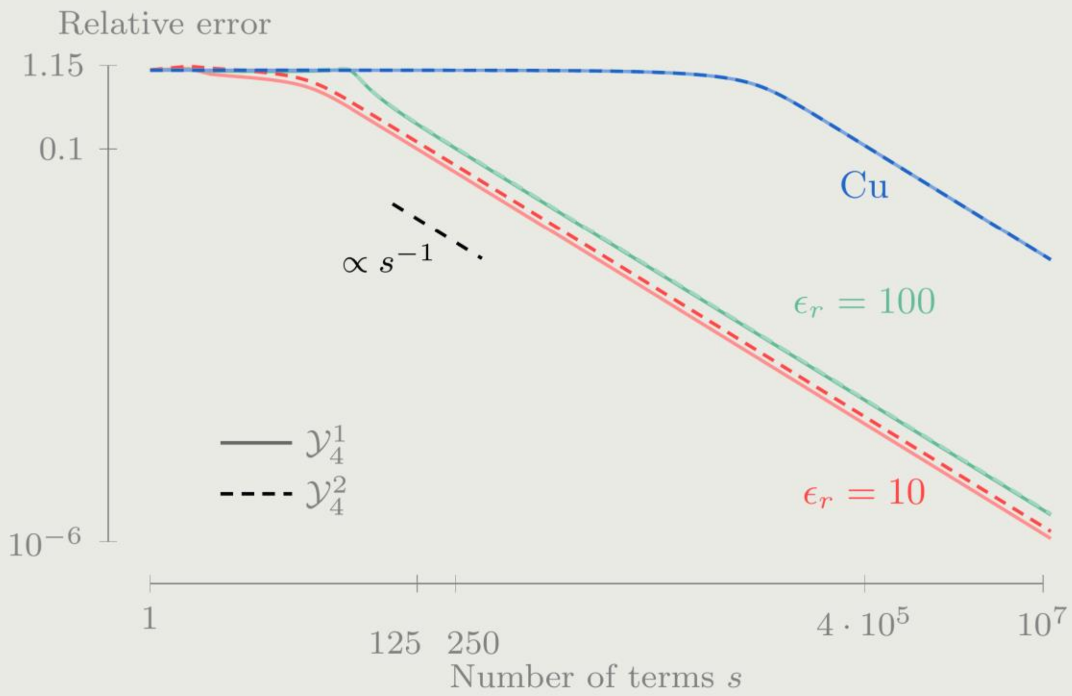


**Solution: closed-form expression** based on generalized Fourier series

# Closed-form DSA elements

## Analytical solution

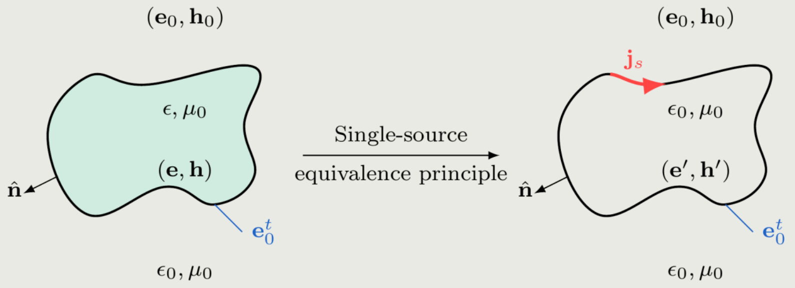


Just like for the conventional Fourier series, the function **f** is projected on a set of orthogonal basis functions

$$f(r) \sim \sum_{s=0}^{\infty} \frac{\langle f, j_n(k_{ns}r)\rangle}{\|j_n(k_{ns}r)\|^2} j_n(k_{ns}r)$$

By choosing the correct **f**, the Fourier sum becomes $\mathcal{Y}_n^{(1)}$ and $\mathcal{Y}_n^{(2)}$

hence their **closed form** is found to be

$$\mathcal{Y}_n^{(1)} \propto \frac{(ka)^2 j_n(ka)}{[ka j_n(ka)]'} - \frac{(k_0 a)^2 j_n(k_0 a)}{[k_0 a j_n(k_0 a)]'}$$

$$\mathcal{Y}_n^{(2)} \propto ka \frac{[ka j_n(ka)]'}{j_n(ka)} - k_0 a \frac{[k_0 a j_n(k_0 a)]'}{j_n(k_0 a)}$$

Leading to **fast**, **accurate** evaluations for the final solution

# Numerical results

## Radial dipole

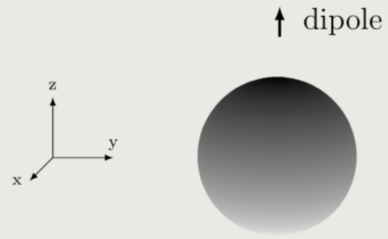


Parameters set-up

- Radius sphere: 1 m
- Distance dipole from origin: 10 m
- Dipole moment: 1 A m
- Frequency: $k_0 = 4\pi$ /1m
- # terms in Mie series: 50
- # terms in DSA-EFIE: 50
- 3 different materials:
    - Low-contrast dielectric
    - High-contrast dielectric
    - Lossy dielectric

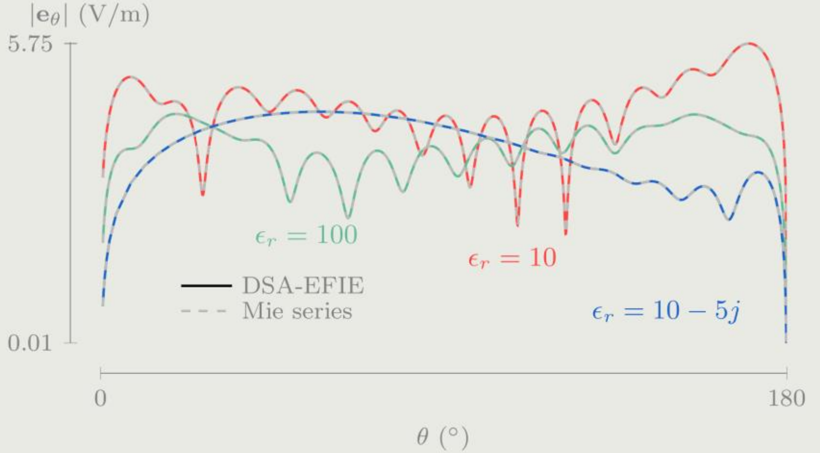


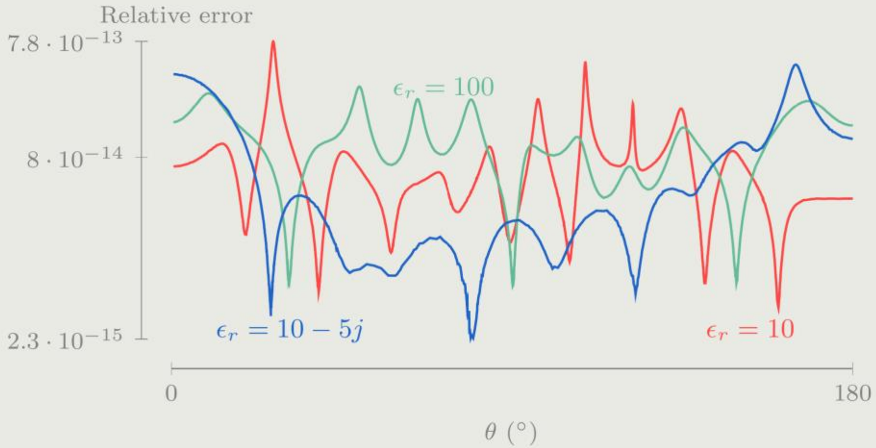


> **12 significant digits** compared to the Mie series so the DSA-EFIE provides a rigorous solution

# Numerical results

## Tangential dipole

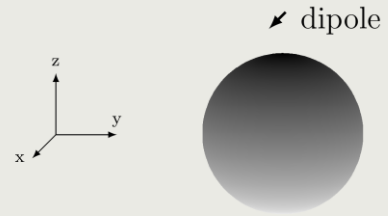


Parameters set-up

- Radius sphere: 1 m
- Distance dipole from origin: 10 m
- Dipole moment: 1 A m
- Frequency: $k_0 = 4\pi$ /1m
- # terms in Mie series: 50
- # terms in DSA-EFIE: 50
- 3 different materials:
    - Low-contrast dielectric
    - High-contrast dielectric
    - Lossy dielectric

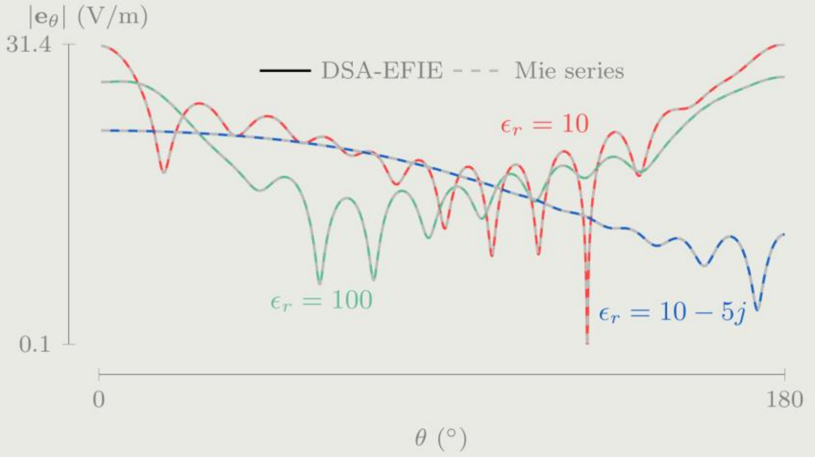


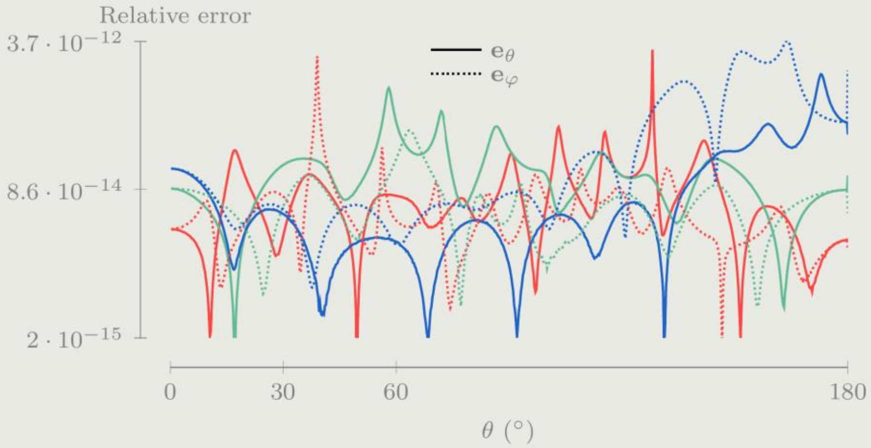


> **12 significant digits** compared to the Mie series so the DSA-EFIE provides a rigorous solution

# Numerical results

## Radial dipole, good conductor

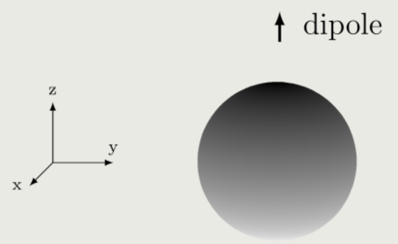


Parameters set-up

- Radius sphere: 1 m
- Distance dipole from origin: 10 m
- Dipole moment: 1 A m
- Frequency: $k_0$ = 4π /1m
- # terms in Mie series: 50
- # terms in DSA-EFIE: 50
- Copper (σ=5,8e7 S/m) from 10 kHz up to 1 GHz
- Observation point at 1 m above the surface for θ= π/4

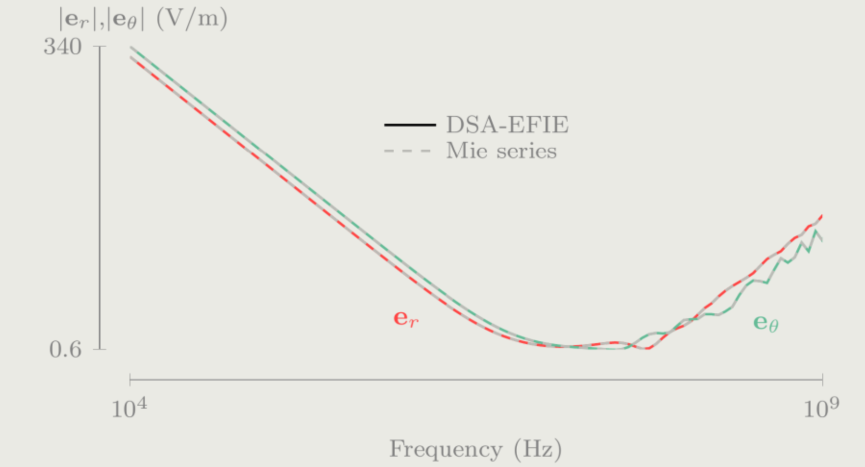



> 15 significant digits compared to the Mie series

so the DSA-EFIE provides a rigorous solution for this difficult-to-handle class of materials

# Spectral analysis

## Dense-mesh breakdown

$\mathcal{Z}_n^{(1)}\mathcal{Y}_n^{(1)}$ and $\mathcal{Z}_n^{(2)}\mathcal{Y}_n^{(2)}$ are the eigenvalues of the DSA-EFIE system

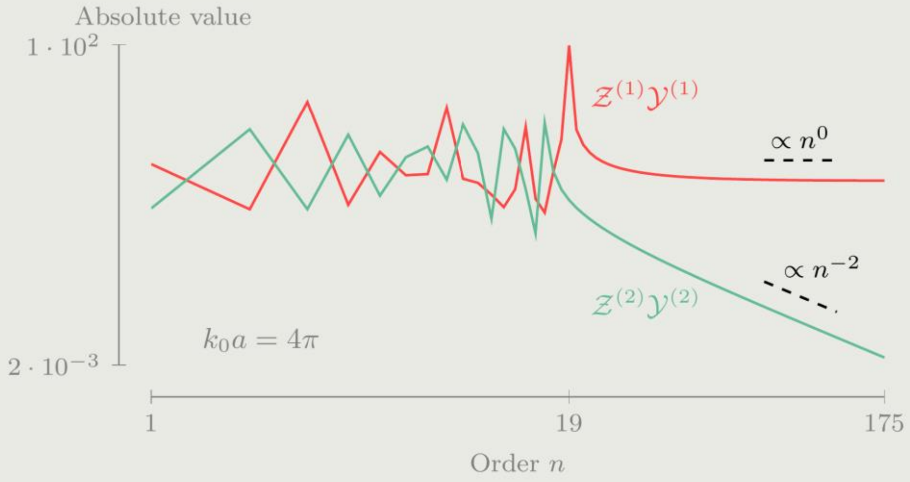


For large n, one set of eigenvalues accumulates at zero, while the other stays constant

this leads to dense-mesh breakdown

Choice of Sobolev space does not solve the issue

**Comparison:**

- EFIE [7] : Sobolev $H^{-1/2}$ (div) testing avoids dense-mesh breakdown
- MFIE [7] : $L^2$ testing avoids dense-mesh breakdown
- SVS-EFIE-J [8]: Sobolev $H^{-1/2}$ (div) testing avoids dense-mesh breakdown
- SVS-EFIE-M [9]: $L^2$ testing avoids dense-mesh breakdown

[7] Hsiao, IEEE TAP 1997    [8] Goni, IEEE TAP 2021    [9] Goni, IEEE JMMCT 2022

# Spectral analysis

## Low-frequency breakdown

$\mathcal{Z}_n^{(1)}\mathcal{Y}_n^{(1)}$ and $\mathcal{Z}_n^{(2)}\mathcal{Y}_n^{(2)}$ are the eigenvalues of the DSA-EFIE system

For small f, one set of eigenvalues accumulates at zero, while the other stays constant

this leads to low-frequency breakdown

Inherent to the EFIE so Sobolev testing space does not solve this issue

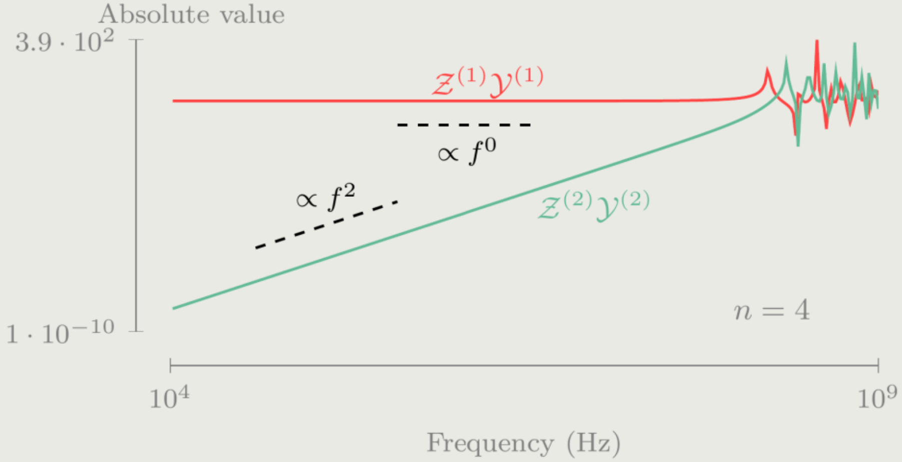


**Comparison:**

- EFIE [7] : Inherent low-frequency breakdown
- MFIE [7] : Absence of low-frequency breakdown
- SVS-EFIE-J [8]: Inherent low-frequency breakdown
- SVS-EFIE-M [9]: Absence of low-frequency breakdown


[7] Hsiao, IEEE TAP 1997

[8] Goni, IEEE TAP 2021

[9] Goni, IEEE JMMCT 2022

# Conclusion

## & future work

We presented an **analytic solution** to the **Differential Surface Admittance** operator combined with the EFIE for scattering at a **sphere**

Analytical solution is **devoid** of any remaining **summation** or **numerical integration** and provides **>12 significant digits**

Spectral analysis confirms **dense-mesh breakdown** and **low-frequency breakdown**

**Future work**

Developed exact **solution** is an excellent **analytical tool** to develop **new DSA-BIE formulations** with preferable properties

quest.
Quantum Mechanical &
Electromagnetic Systems
Modelling Lab

GHENT UNIVERSITY
imec

Technologiepark – Zwijnaarde 126, B-9052 Gent, Belgium
**Martijn.huynen@ugent.be**
**www.QuestLab.be**

Martijn HUYNEN, Post-doctoral researcher